

## Pressure Analysis of a Vertical Well: Implementing Source and Green Functions

Adookor Wisdom Suanu, Otamere Blessing and Mamudu Abbas

Department of Petroleum Engineering, University of Benin, Nigeria.

### Abstract

Identification of reservoir boundaries and their effects on pressure distribution assist in defining and managing the reservoir system. In this paper, Pressure distribution study in a vertical well system is carried out by analyzing the effects of the intrinsic reservoir parameters on the pressure distribution such as  $Z_D$ ,  $X_D$  and  $X_{eD}$  representing the vertical point coordinate, lateral point coordinate and lateral extent respectively. Approximated source and green functions approach was used. The results show that infinite – acting flow period subsists for a long time when flow is close to the well bore, thereby making it possible to accurately determine near – well bore characteristics using the conventional analysis procedures such as buildup, drawdown and or any other procedure. The vertical point coordinates which connotes a position along the reservoir thickness affects the time of attainment of pseudo – steady state. The impact of the boundaries on pressure responses occur at late time production. Pressure behaviors at early time production are not affected by the boundaries. Pressure behavior of a vertical well in a bounded reservoir is affected significantly by the reservoir boundary. Furthermore, it was observed that the infinite – acting flow period is unaffected by the lateral extent of the reservoir.

**Keywords:** Bounded Reservoir, Dimensionless Pressure, Dimensionless Pressure Derivative, Lateral Extent, Lateral Point Coordinate, Log – Log Plot, Reservoir Boundaries, Pressure Distribution, Reservoir Thickness, Vertical Point Coordinate and Vertical Well

#### Nomenclature

$p_D$  = Dimensionless pressure.  
 $h_D$  = Dimensionless reservoir thickness.  
 $x_D$  = Point co-ordinate along the X – direction.  
 $z_D$  = Point co-ordinate along the Z – direction.  
S = Source function.  
 $\tau$  = Time.  
 $t_D$  = Dimensionless time  
 $x_{ed}$  = Reservoir lateral extent.  
k = Reservoir permeability  
ct = Total compressibility  
 $\mu$  = Viscosity  
 $\phi$  = Porosity

### 1.0 Introduction

The analysis of pressure data has been a subject of interest to petroleum engineers for many decades. Pressure data can be analyzed to determine reservoir parameters and flow characteristics. Measurement of bottom hole pressure data is one of the few ways of acquiring “real time” data can be obtained with a high degree of accuracy for a very reasonable cost. Hence there is much interest in acquiring and interpreting pressure data. Throughout the life of an oil well, from exploration to abandonment, a sufficient amount of well test data are collected to describe well condition and behavior. It should be emphasized that the multidisciplinary professionals need to work as an integrated team to develop and implement the well test data management program with efficacious models. Well test pressure responses characterize the ability of the fluid to flow

---

Corresponding author: Adookor W. Suanu, E-mail: Wisado99@yahoo.com, Tel.: +2348035713489 & 07053042686 (O.B)

through the reservoir and to the well. Tests provide a description of the reservoir in dynamic conditions, as opposed to geological and log data.

## 2.0 Problem Definition

Identification of reservoir boundaries and their effects on pressure distribution assist in defining and managing the reservoir system. The dependence on long aged established mathematical models has limited the extent of pressure distribution analysis that can be done during well test analysis under some circumstances. This leads to the advances in the use of numerical modeling approach in pressure distribution analysis as implemented in this research.

## 3.0 Technical Objective

The objectives of this research include:

1. To simulate the actual reservoir behavior using numerical mathematical models derived from Source and Green functions.
2. To determine the various flow regimes.
3. To delineate the appropriate flow periods.
4. To analyze the effect of wellbore and reservoir parameters on the pressure behavior in a bounded reservoir.
5. To study the pressure distribution of the reservoir at various dimensionless times.

## 4.0 Literature Review

Well test analysis became a true reservoir characterization tool decades ago. Researches carried out on daily basis till date has made it one of the major tool used in reservoir evaluation. Good number of innovative researches could be found in the literature [1-10]. Oloro and Adewole [8] gave an analysis using Source and Green's Function, the Factors that Affect Pressure Distribution of Horizontal Wells in a Layered Reservoir with Simultaneous Gas – cap and Bottom Water Drive. Owolabi et al. [9] presented the use of Source and Green's Function in Pressure Distribution in a Layered Reservoir with Gas – cap and Bottom Water. Extensive researches have been reported by several researchers on Transient Pressure Analysis of Horizontal Wells including an extensive research on pressure drawdown and buildup analysis of horizontal wells in anisotropic media [11 – 14]. Despite the fact that advances in well testing have resulted in several research works over the past decades, approximating the use of Source and Green's Function in Pressure Distribution in vertical well testing is not common among researches carried out today. This has been tested in this work.

## 5.0 Flow Regimes Categories [15]

At different times, fluid flows in the reservoir with different ways generally based on the shape and size of the reservoir. Flow behavior classification is studied in terms of pressure rate of change with respect to time. Three main flow regimes will be described in this sub-chapter; they are steady-state flow, pseudo steady state flow, and transient state flow.

## 6.0 Steady State Flow [15]

In steady state flow, there is no pressure change anywhere with time (Equation (1)). It occurs during the late time region when the reservoir has gas cap or aquifer support. This condition is also called constant pressure boundary which pressure maintenance might apply in the producing formation.

$$\frac{\partial p}{\partial t} = 0 \dots\dots\dots (1)$$

## 7.0 Pseudo Steady State Flow [15]

This flow regime also occurs in late-time region, but it forms when there is no flow in the reservoir outer boundaries. No flow boundaries can be caused by the effect of nearby producing or presence of sealing faults. It is a closed system or acts as a tank where a constant rate production results constant pressure drop for each unit of time (Equation (2)). This flow is also called semi-steady state or depletion state.

$$\frac{\partial p}{\partial t} = \text{constant} \dots\dots\dots (2)$$

## 8.0 Transient State Flow [16]

When the pressure/rate changes with time due to well geometry and the reservoir properties (i.e. permeability and heterogeneity), it indicates that transient (unsteady state) flow occurs (Equation (3)). It is observed before boundary effects are reached or also called infinite acting time period. Higher compressibility of the fluid leads the more pronounced the unsteady state effect of the reservoir fluid.

$$\frac{\partial p}{\partial t} = f(x, y, t) \dots \dots \dots (3)$$

**9.0 Radius of investigation [16]**

Quantitatively and qualitatively, radius of investigation has great significance both in planning and analyzing a well test. It describes the distance (from the tested wellbore) of the transient pressure into the formation if there is an unstable pressure caused by production or closure of a well. It will show that this distance has a correlation with physical properties of the rock and fluid and also depends on the length of time of well testing.

There is a time *t* when the pressure disturbance reaches the distance *r<sub>i</sub>*(radius of investigation). The relationship between *t* and *r<sub>i</sub>* is given by;

$$r_i = \left( \frac{kt}{9480\mu c_t} \right)^{0.5} \dots \dots \dots (4)$$

From equation above, *r<sub>i</sub>* describes a distance at which the pressure disturbance (increase or decrease) simply influences due to production or injection of fluid at constant rate.

**10.0 Methodology**

This section presents the derived models and their applications, representing a vertical well in a bounded reservoir for lateral extent and point coordinate effects on the pressure distributions analysis.

In this research, the following assumptions about the well and reservoir being modeled were made in developing the bounded reservoir model.

- The reservoir is homogeneous
- The reservoir is rectangular in shape
- The reservoir is anisotropic
- The boundaries in a given axis are felt by the transient pressure at the same time

In developing the mathematical equation representing the above described model, the Source and Green’s function expression and the Newman’s product rule were employed to determine the dimensionless pressure analysis.

Newman’s product rule is expressed as:

$$S(x_D, z_D, t_D) = S(x_D, t_D) \cdot S(z_D, t_D) \dots \dots \dots (5)$$

And the dimensionless pressure response is expressed as:

$$p_D = 2\pi h_D \int_0^{t_D} S(x_D, \tau) \cdot S(z_D, \tau) d\tau \dots \dots \dots (6)$$

*a. Dimensionless Pressure Models*

The analytical models for the transient pressure response of a vertical well in a bounded reservoir are expressed below

*b. Early Time Flow Period*

This is an infinite-acting period when the transient pressure has not felt any boundaries. The required source function expressions for this flow period as read from the source function table are as follows:

$$S(x, t) = \frac{1}{2\sqrt{\eta_x \pi t}} e^{-\frac{(x-x_w)^2}{4\eta_x t}} \dots \dots \dots (8)$$

Source is an infinite plane source in an infinite reservoir

Source function number: I(X)

$$S(z, t) = \frac{1}{2\sqrt{\eta_z \pi t}} e^{-\frac{(z-z_w)^2}{4\eta_z t}} \dots \dots \dots (9)$$

Source is an infinite plane source in an infinite reservoir

Source function number: I(Z)

In dimensionless form;

$$S(x_D, t_D) = \frac{1}{2\sqrt{\pi t_D}} \sqrt{\frac{k}{k_x}} e^{-\frac{(x_D-x_{wD})^2}{4t_D}} \dots \dots \dots (10)$$

$$S(z_D, t_D) = \frac{1}{2\sqrt{\pi t_D}} \sqrt{\frac{k}{k_z}} e^{-\frac{(z_D-z_{wD})^2}{4t_D}} \dots \dots \dots (11)$$

Using the Newman’s product method, the model for the dimensionless pressure response of a vertical well during the early radial flow period is given as;

Substituting equations (9) and (10) into equation (6) gives

$$p_D = -\frac{1}{2} \frac{k}{\sqrt{k_x k_z}} \int_0^{t_D} \frac{e^{-[(x_D-x_{wD})^2 + (z_D-z_{wD})^2]/4\tau}}{\tau} d\tau \dots \dots \dots (12)$$

*c. First Transition Time Flow Model*

In the first transition time flow model, the boundaries in the x - direction have been seen while the boundaries in the z - direction have not been seen by the well. The required source functions as read from the source function Table as follows:

$$S(x, t) = \frac{1}{x_e} \left[ 1 + 2 \sum_{i=1}^n \exp \left( -\frac{n^2 \pi^2 \eta_x t}{x_e^2} \right) \cos n\pi \frac{x_w}{x_e} \cos n\pi \frac{x}{x_e} \right] \dots \dots \dots (13)$$

Source is an infinite plane source in an infinite slab reservoir  
Source function number: VII (X)

$$S(z, t) = \frac{1}{2\sqrt{\eta_z \pi t}} e^{\left[ -\frac{(z-z_w)^2}{4\eta_z t} \right]} \dots \dots \dots (14)$$

Source is an infinite plane source in an infinite reservoir.  
Source function number: I(Z)

In dimensionless form;

$$S(x_D, t_D) = \frac{1}{x_{eD}} \sqrt{\frac{k}{k_x}} \left[ 1 + 2 \sum_{i=1}^n \exp \left( -\frac{n^2 \pi^2 t_D}{x_{eD}^2} \right) \cos n\pi \frac{x_{wD}}{x_{eD}} \cos n\pi \frac{x_D}{x_{eD}} \right] \dots \dots \dots (15)$$

$$S(z_D, t_D) = \frac{1}{2\sqrt{\pi t_D}} \sqrt{\frac{k}{k_z}} e^{\left[ -\frac{(z_D-z_{wD})^2}{4t_D} \right]} \dots \dots \dots (16)$$

Using the Newman's product method, the model for the dimensionless pressure response of a vertical well during the intermediate flow period is given as;

Substituting equations (14) and (15) into equation (6)

$$p_D = \frac{k}{\sqrt{k_x k_z}} \frac{\pi h_D}{x_{eD}} \int_{t_{De}}^{t_{D1}} \left[ 1 + 2 \sum_{i=1}^n \exp \left( -\frac{n^2 \pi^2 \tau}{x_{eD}^2} \right) \cos n\pi \frac{x_{wD}}{x_{eD}} \cos n\pi \frac{x_D}{x_{eD}} \right] \times \frac{1}{\sqrt{\tau}} e^{\left[ -\frac{(z_D-z_{wD})^2}{4\tau} \right]} d\tau. (17)$$

d. Second Transition Time Flow Model

In the second transition time flow model, the boundaries in the z - direction have been seen while the boundaries in the x - direction have not been seen by the well. The required source functions as read from the source function table are as follows:

$$S(x, t) = \frac{1}{2\sqrt{\eta_x \pi t}} e^{\left[ -\frac{(x-x_w)^2}{4\eta_x t} \right]} \dots \dots \dots (18)$$

Source is an infinite plane source in an infinite reservoir.  
Source function number: I(X)

$$S(z, t) = \frac{1}{z_e} \left[ 1 + 2 \sum_{i=1}^n \exp \left( -\frac{n^2 \pi^2 \eta_z t}{z_e^2} \right) \cos n\pi \frac{z_w}{z_e} \cos n\pi \frac{z}{z_e} \right] \dots \dots \dots (19)$$

Source is an infinite plane source in an infinite slab reservoir.  
Source function number: VII (Z)

In dimensionless form;

$$S(x_D, t_D) = \frac{1}{2\sqrt{\pi t_D}} \sqrt{\frac{k}{k_x}} e^{\left[ -\frac{(x_D-x_{wD})^2}{4t_D} \right]} \dots \dots \dots (20)$$

$$S(z_D, t_D) = \frac{1}{h_D} \sqrt{\frac{k}{k_z}} \left[ 1 + 2 \sum_{i=1}^n \exp \left( -\frac{n^2 \pi^2 t_D}{h_D^2} \right) \cos n\pi \frac{z_{wD}}{h_D} \cos n\pi \frac{z_D}{h_D} \right] \dots \dots \dots (21)$$

Using the Newman's product method, the model for the dimensionless pressure response of a vertical well during the intermediate flow period is given as;

Substituting equations (19) and (20) into equation (6)

$$p_D = \frac{k}{\sqrt{k_x k_z}} \pi \int_{t_{D1}}^{t_{D2}} \left[ 1 + 2 \sum_{i=1}^n \exp \left( -\frac{n^2 \pi^2 \tau}{h_D^2} \right) \cos n\pi \frac{z_{wD}}{h_D} \cos n\pi \frac{z_D}{h_D} \right] \times \frac{1}{\sqrt{\tau}} e^{\left[ -\frac{(x_D-x_{wD})^2}{4\tau} \right]} d\tau \dots \dots (22)$$

e. Late Time Flow Model

In this case, the boundaries in both the X and z directions have been felt. The required source function expressions as read from the source function table are as follows:

$$S(x, t) = \frac{1}{x_e} \left[ 1 + 2 \sum_{i=1}^n \exp \left( -\frac{n^2 \pi^2 \eta_x t}{x_e^2} \right) \cos n\pi \frac{x_w}{x_e} \cos n\pi \frac{x}{x_e} \right] \dots \dots \dots (23)$$

Source is an infinite plane source in an infinite slab reservoir  
Source function number: VII (X)

$$S(z, t) = \frac{1}{z_e} \left[ 1 + 2 \sum_{i=1}^n \exp \left( -\frac{n^2 \pi^2 \eta_z t}{z_e^2} \right) \cos n\pi \frac{z_w}{z_e} \cos n\pi \frac{z}{z_e} \right] \dots \dots \dots (24)$$

Source is an infinite plane source in an infinite slab reservoir  
Source function number: VII (Z)

In dimensionless form;

$$S(x_D, t_D) = \frac{1}{x_{eD}} \sqrt{\frac{k}{k_x}} \left[ 1 + 2 \sum_{i=1}^n \exp \left( -\frac{n^2 \pi^2 t_D}{x_{eD}^2} \right) \cos n\pi \frac{x_{wD}}{x_{eD}} \cos n\pi \frac{x_D}{x_{eD}} \right] \dots \dots \dots (25)$$

$$S(z_D, t_D) = \frac{1}{h_D} \sqrt{\frac{k}{k_z}} \left[ 1 + 2 \sum_{i=1}^n \exp \left( -\frac{n^2 \pi^2 t_D}{h_D^2} \right) \cos n\pi \frac{z_{wD}}{h_D} \cos n\pi \frac{z_D}{h_D} \right] \dots \dots \dots (26)$$

Using the Newman’s product method, the model for the dimensionless pressure response of a vertical well during the late time flow period is given as;

Substituting equations (24) and (25) into equation (6) gives

$$p_D = \frac{k}{\sqrt{k_x k_z}} \frac{2\pi}{x_{eD}} \int_{t_{D2}}^{t_{D3}} \left[ 1 + 2 \sum_{i=1}^n \exp\left(\frac{-n^2 \pi^2 \tau}{x_{eD}^2}\right) \cos n\pi \frac{x_{wD}}{x_{eD}} \cos n\pi \frac{x_D}{x_{eD}} \right] \times \left[ 1 + 2 \sum_{i=1}^n \exp\left(\frac{-n^2 \pi^2 \tau}{h_D^2}\right) \cos n\pi \frac{z_{wD}}{h_D} \cos n\pi \frac{z_D}{h_D} \right] d\tau \dots\dots\dots (27a)$$

The sum of all the dimensionless pressure equations (equations (11), (16), (21) and (26) for all the flow periods is expressed in equation (27b).

$$p_D = -\pi \frac{k}{\sqrt{k_x k_z}} \left\{ \frac{1}{2} \int_0^{t_{De}} \frac{e^{-[(x_D-x_{wD})^2+(z_D-z_{wD})^2]/4\tau}}{\tau} - \left[ \frac{h_D}{x_{eD}} \int_{t_{De}}^{t_{D1}} \left[ 1 + 2 \sum_{i=1}^n \exp\left(-\frac{n^2 \pi^2 \tau}{x_{eD}^2}\right) \cos n\pi \frac{x_{wD}}{x_{eD}} \cos n\pi \frac{x_D}{x_{eD}} \right] \times \frac{1}{\sqrt{\tau}} e^{-\left[\frac{(z_D-z_{wD})^2}{4\tau}\right]} - \left[ \int_{t_{D1}}^{t_{D2}} \left[ 1 + 2 \sum_{i=1}^n \exp\left(-\frac{n^2 \pi^2 \tau}{h_D^2}\right) \cos n\pi \frac{z_{wD}}{h_D} \cos n\pi \frac{z_D}{h_D} \right] \times \frac{1}{\sqrt{\tau}} e^{-\left[\frac{(x_D-x_{wD})^2}{4\tau}\right]} - \left\langle \frac{2}{x_{eD}} \int_{t_{D2}}^{t_{D3}} \left[ 1 + 2 \sum_{i=1}^n \exp\left(\frac{-n^2 \pi^2 \tau}{x_{eD}^2}\right) \cos n\pi \frac{x_{wD}}{x_{eD}} \cos n\pi \frac{x_D}{x_{eD}} \right] \times \left[ 1 + 2 \sum_{i=1}^n \exp\left(\frac{-n^2 \pi^2 \tau}{h_D^2}\right) \cos n\pi \frac{z_{wD}}{h_D} \cos n\pi \frac{z_D}{h_D} \right] \dots\dots\dots (27b)$$

f. Solutions to Flow Equations

g. Dimensionless Pressure:

h. Early Time Flow

Using the Gauss-Laguerre quadrature, the early radial flow equation (equation (11)) can be expressed as:

$$p_D = -\frac{1}{2} \frac{k}{\sqrt{k_x k_z}} E_i \left[ -\frac{(x_D-x_{wD})^2+(z_D-z_{wD})^2}{4t_D} \right] \dots\dots\dots (28)$$

i. First Transition Time Flow

Using the Gauss - Legendre quadrature, the first transition time flow equation (equation 16) can be expressed as:

$$p_D = \frac{\pi h_D}{x_{eD}} \frac{k}{\sqrt{k_x k_z}} \left(\frac{b-a}{2}\right) \sum_{i=1}^n w_i f \left[ 1 + 2 \exp\left\langle \frac{-n^2 \pi^2}{x_{eD}^2} \left(\frac{z_i(b-a)+b+a}{2}\right) \right\rangle \cdot \cos n\pi \frac{x_{wD}}{x_{eD}} \cos n\pi \frac{x_D}{x_{eD}} \right] \times \frac{\exp\left[-\frac{(z_D-z_{wD})^2}{4\left(\frac{z_i(b-a)+b+a}{2}\right)}\right]}{\sqrt{\left(\frac{z_i(b-a)+b+a}{2}\right)}} \dots\dots\dots (29)$$

j. Second Transition Time Flow

Using the Gauss - Legendre quadrature, the second transition time flow equation (equation 5.17) can be expressed as:

$$p_D = \frac{\pi k}{\sqrt{k_x k_z}} \left(\frac{b-a}{2}\right) \sum_{i=1}^n w_i f \left[ 1 + 2 \exp\left\langle \frac{-n^2 \pi^2}{h_D^2} \left(\frac{z_i(b-a)+b+a}{2}\right) \right\rangle \cdot \cos n\pi \frac{z_{wD}}{H_D} \cos n\pi \frac{z_D}{H_D} \right] \times \frac{\exp\left[-\frac{(x_D-x_{wD})^2}{4\left(\frac{z_i(b-a)+b+a}{2}\right)}\right]}{\sqrt{\left(\frac{z_i(b-a)+b+a}{2}\right)}} \dots\dots\dots (30)$$

k. Late Time Flow

Using the Gauss - Legendre quadrature, the late time flow can be expressed as:

$$p_D = \frac{2\pi}{x_{eD}} \frac{k}{\sqrt{k_x k_z}} \left(\frac{b-a}{2}\right) \sum_{i=1}^n w_i f \left\{ \left[ 1 + 2 \exp\left\langle \frac{-n^2 \pi^2}{x_{eD}^2} \left(\frac{z_i(b-a)+b+a}{2}\right) \right\rangle \right] \cos n\pi \frac{x_{wD}}{x_{eD}} \cos n\pi \frac{x_D}{x_{eD}} \right\} \times \left[ 1 + 2 \exp\left\langle \frac{-n^2 \pi^2}{h_D^2} \left(\frac{z_i(b-a)+b+a}{2}\right) \right\rangle \cdot \cos n\pi \frac{z_{wD}}{h_D} \cos n\pi \frac{z_D}{h_D} \right] \dots\dots\dots (31)$$

l. Dimensionless Pressure Derivative:

m. Early Time Flow

The dimensionless pressure derivative at early – time flow can be expressed as:

$$p'_D = \frac{1}{2} \frac{k}{\sqrt{k_x k_z}} \exp \left[ -\frac{(x_D - x_{wD})^2 + (z_D - z_{wD})^2}{4t_D} \right] \dots \dots \dots (32)$$

n. First Transition Time Flow

The dimensionless pressure derivative at first transition - time flow can be expressed as:

$$p'_D = \frac{t_D \pi h_D}{x_{eD}} \frac{k}{\sqrt{k_x k_z}} \sum_{i=1}^n \left[ 1 + 2 \exp \left\langle \frac{-n^2 \pi^2 t_D}{x_{eD}^2} \right\rangle \cdot \cos n \pi \frac{x_{wD}}{x_{eD}} \cos n \pi \frac{x_D}{x_{eD}} \right] \times \frac{\exp \left[ -\frac{(z_D - z_{wD})^2}{4t_D} \right]}{\sqrt{t_D}} \dots \dots \dots (33)$$

o. Second Transition Time Flow

The dimensionless pressure derivative at second transition – time flow can be expressed as:

$$p'_D = t_D \pi \frac{k}{\sqrt{k_x k_z}} \sum_{i=1}^n \left[ 1 + 2 \exp \left\langle \frac{-n^2 \pi^2 t_D}{h_D^2} \right\rangle \cdot \cos n \pi \frac{z_{wD}}{H_D} \cos n \pi \frac{z_D}{H_D} \right] \times \frac{\exp \left[ -\frac{(x_D - x_{wD})^2}{4t_D} \right]}{\sqrt{t_D}} \dots \dots \dots (34)$$

p. Late Time Flow

The dimensionless pressure derivative at late – time flow can be expressed as:

$$p'_D = \frac{t_D 2\pi}{x_{eD}} \frac{k}{\sqrt{k_x k_z}} \sum_{i=1}^n \left\{ \left[ 1 + 2 \exp \left\langle \frac{-n^2 \pi^2 t_D}{x_{eD}^2} \right\rangle \cos n \pi \frac{x_{wD}}{x_{eD}} \cos n \pi \frac{x_D}{x_{eD}} \right] \times \left[ 1 + 2 \exp \left\langle \frac{-n^2 \pi^2 t_D}{h_D^2} \right\rangle \cos n \pi \frac{z_{wD}}{h_D} \cos n \pi \frac{z_D}{h_D} \right] \right\} \dots \dots \dots (35)$$

q. Flow Time Equations and Solutions

These equations are presented here for estimating the various flow regimes based on the concept of Odeh and Babu[13].

r. Early Time Flow

The duration of this flow period may be approximated by the minimum of the two following terms

$$t_{e1} = \frac{1800 d_z^2 \phi \mu c_t}{k_v} \dots \dots \dots (36)$$

And

$$t_{e1} = \frac{125 L^2 \phi \mu c_t}{k_v} \dots \dots \dots (37)$$

Where  $d_z$  is the shortest distance between the well and the z – boundary.

Dimensionless time is expressed as:

$$t_D = \frac{0.00264 k t}{\phi \mu c_t r_w^2} \dots \dots \dots (38)$$

Substituting separately equations (36) and (37) into equation (38) gives:

$$t_{De} = \frac{4.752 (h - z_w)^2}{k_v r_w^2} \dots \dots \dots (39)$$

And

$$t_{De} = 0.33 \frac{k}{k_v} \dots \dots \dots (40)$$

Therefore, the duration of the early time radial flow period may be approximated by the minimum of the following two terms

$$t_{De} = \frac{4.752 (h - z_w)^2}{k_v r_w^2} \text{ And } t_{De} = 0.33 \frac{k}{k_v} \dots \dots \dots (41)$$

s. First Transition Flow Time

The time for this flow starts at

$$t_{e1} = \frac{1800 \phi D_z^2 \mu c_t}{k_v} \dots \dots \dots (42)$$

And ends at

$$t_{e2} = \frac{160L^2\phi\mu c_t}{k_x} \dots\dots\dots (43)$$

Where  $Dz$  is the longest distance between the well and the  $z$  – boundary.

Substituting separately equations (42) and (43) into equation (38) gives:

$$t_{D1} = \frac{4.752(h-z)^2}{k_v r_w^2} \dots\dots\dots (44)$$

And

$$t_{D2} = 0.4224 \frac{k}{k_x} \dots\dots\dots (45)$$

Therefore, the first transition time flow starts at

$$t_{D1} = \frac{4.752(h-z)^2}{k_v r_w^2} \text{ And ends at } t_{D2} = 0.4224 \frac{k}{k_x} \dots\dots\dots (46)$$

*t. Second Transition Flow Time*

The time for this flow starts at

$$t_{e3} = \frac{1480r_w^2\phi\mu c_t}{k_x} \dots\dots\dots (47)$$

And ends at

$$t_{e3} = \frac{2000\phi\mu c_t(d_x + \frac{r_w}{4})^2}{k_x} \dots\dots\dots (48)$$

Where  $dx$  is the shortest distance between the well and the  $z$  – boundary, ft.

Substituting separately equations (47) and (48) into equation (38) gives:

$$t_{D3} = 3.9072 \frac{k}{k_x} \dots\dots\dots (49)$$

And

$$t_{D4} = \frac{5.28k((x_e-x) + \frac{r_w}{4})^2}{k_x} \dots\dots\dots (50)$$

Therefore, the second transition time flow starts at

$$t_{D3} = 3.9072 \frac{k}{k_x} \text{ And ends at } t_{D4} = \frac{5.28k((x_e-x) + \frac{r_w}{4})^2}{k_x} \dots\dots\dots (51)$$

*v. Late Time Flow*

This flow period ends at a maximum of

$$t_{e4} = \frac{4800\phi\mu c_t D_x^2}{k_x} \dots\dots\dots (52)$$

And

$$t_{e4} = \frac{1800\phi D_z^2 \mu c_t}{k_z} \dots\dots\dots (53)$$

Where  $Dx$  is the longest distance between the well and the  $X$  – boundary.

Substituting equations (52) and (53) into equation (38) gives:

$$t_{D5} = \frac{12.67k(x_e-x_w)^2}{k_x r_w^2} \dots\dots\dots (54)$$

And

$$t_{D5} = \frac{4.752(h-z)^2}{k_z r_w^2} \dots\dots\dots (55)$$

Therefore, the late time flow period ends at a maximum of

$$t_{D5} = \frac{5.0688(x_e-x_w)^2}{L^2} \text{ And } t_{D5} = \frac{1.9008(h-z_w)^2}{L^2} \dots\dots\dots (56)$$

**11.0 Results and Discussion**

This section presents the results of the analysis of the effect of well and reservoir parameters on the pressure behavior of a vertical well in a bounded reservoir model. Results of the dimensionless pressure and dimensionless pressure derivatives were obtained using a program Visual Basic 2010. The dimensionless pressure and dimensionless pressure derivative results were then plotted and subsequently analyzed.

*1. Effect Of Vertical Point Coordinate (ZD)*

The effect of the parameter,  $z_D$ , on pressure distribution of a vertical well in a bounded reservoir system was examined by keeping all other parameters constant while varying  $z_D$ .

The vertical point coordinates being varied for the first set of wellbore and reservoir and rock parameters were taken as  $z_D = 1.94$  and  $z_D = 1.923$ .  $z_D = 1.923$  represents a position within the well bore region while  $z_D = 1.94$  represents a position slightly

beyond the well region, close to the lower boundary.

A plot of the dimensionless pressure and dimensionless pressure derivative results against the dimensionless time is also illustrated in Figure 1 on the log-log axis for the first set of parameters.

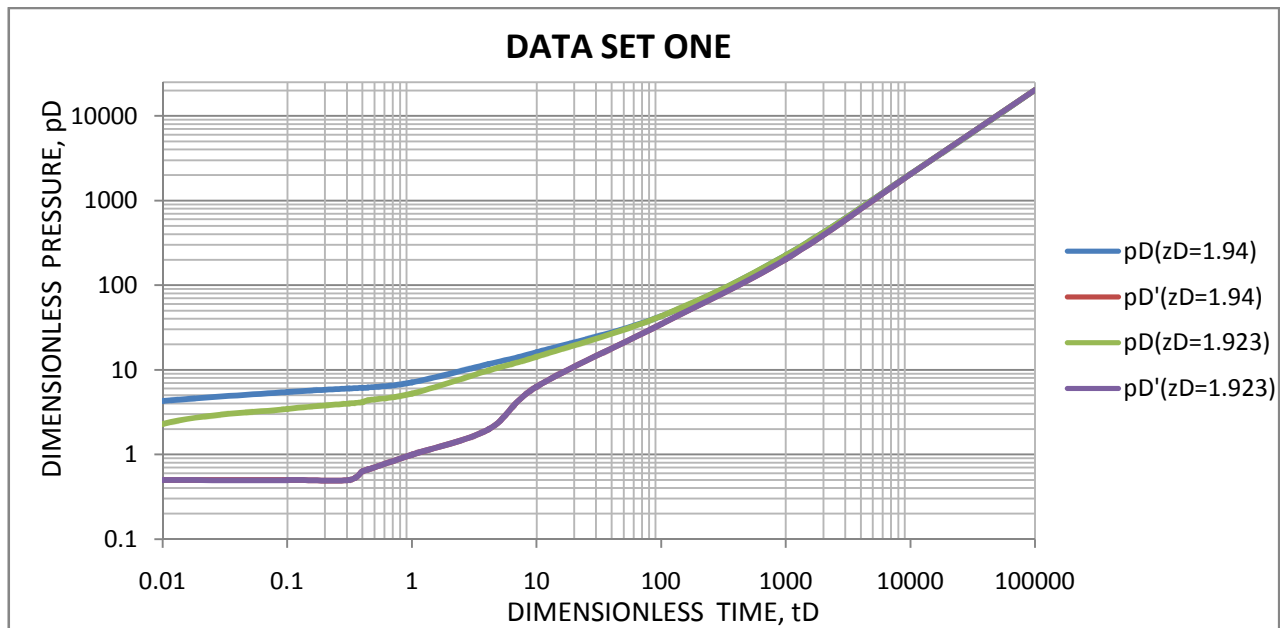


**Figure 1:** Dimensionless Pressure and Dimensionless Pressure Derivative plots for Vertical Point Coordinate Values (Set One)

It can be observed from the plot in Figure 1 that the dimensionless pressure curves for both varied values of  $z_D = 1.923$  and  $z_D = 1.94$  increase infinitely with time with each having a characteristic slope of 1.151 between  $t_D = 0.001$  and  $t_D = 0.313$ . At this point, there is minimal separation between the two curves, signifying that the vertical point coordinate is negligibly small to affect distribution during the early - time flow. During this period flow which is called infinite - acting or radial flow period, the reservoir behaves as though it is extremely large with infinite production. Since the influence of the boundary has not been felt at this time, near - well bore characterization is possible and clean oil production guaranteed. Between  $t_D = 0.313$  and  $t_D = 0.445$ , the reservoir experiences its first transition from the early - time flow signifying the influence of a boundary. At this time, the early - time flow ends and the first transition flow becomes dominant. This flow period indicates that the well has seen the closest boundary either in the x or z plane. This flow is characterized by a smooth transition on the dimensionless pressure curves. The second transition flow occurs between  $t_D = 0.445$  and  $t_D = 4.118$ . This flow period is characterized by a slight deviation in course from the first transition flow pattern on the dimensionless pressure curves. This flow period occurs with the assumption that the boundary that was not seen during the first transition flow is now being seen while the other becomes unseen. The curves remain inseparable throughout the period of transition, thereby indicating that pressure response is unaffected by the vertical point coordinate during this flow period. From the time  $t_D = 4.118$  and upward, pseudo - steady state occurs. It can be seen on the plot, that during this period of flow, the curves rise steadily with increasing pressure values. This pressure increase indicates that the average reservoir pressure of the reservoir system has started to decrease over time; however, pressure distribution remains unaffected by variation in  $z_D$ .

The dimensionless pressure derivative curves as illustrated on the same graph above shows that for both varied values of  $z_D = 1.923$  and  $z_D = 1.94$ , the curves flatten at an approximately constant value of 0.5 during the early - time flow between  $t_D = 0.001$  and  $t_D = 0.313$ . This is usually the norm for a vertical well pressure distribution. Between the early time flow and the first transition flow, the curves experience a visible rise as the influence of a boundary is felt. Between the first and second transition flow, there is a slight dip on the curves. These features are clearly visible on the derivative curves because they reveal features that are hidden in the dimensionless pressure curves.

The vertical point coordinates being varied for the second set of wellbore and reservoir and rock parameters were taken as  $z_D = 3.86$ ,  $z_D = 3.874$  and  $z_D = 3.93$ .  $z_D = 3.86$  represents a position within the well bore region,  $z_D = 3.874$  represents a position slightly beyond the well region, close to the boundary, while  $z_D = 3.93$  represents a position further away from the well region and closer to the boundary.

A plot of the dimensionless pressure and dimensionless pressure derivative results against the dimensionless time is also illustrated in Figure 2 on the log-log axis for the second set of parameters.



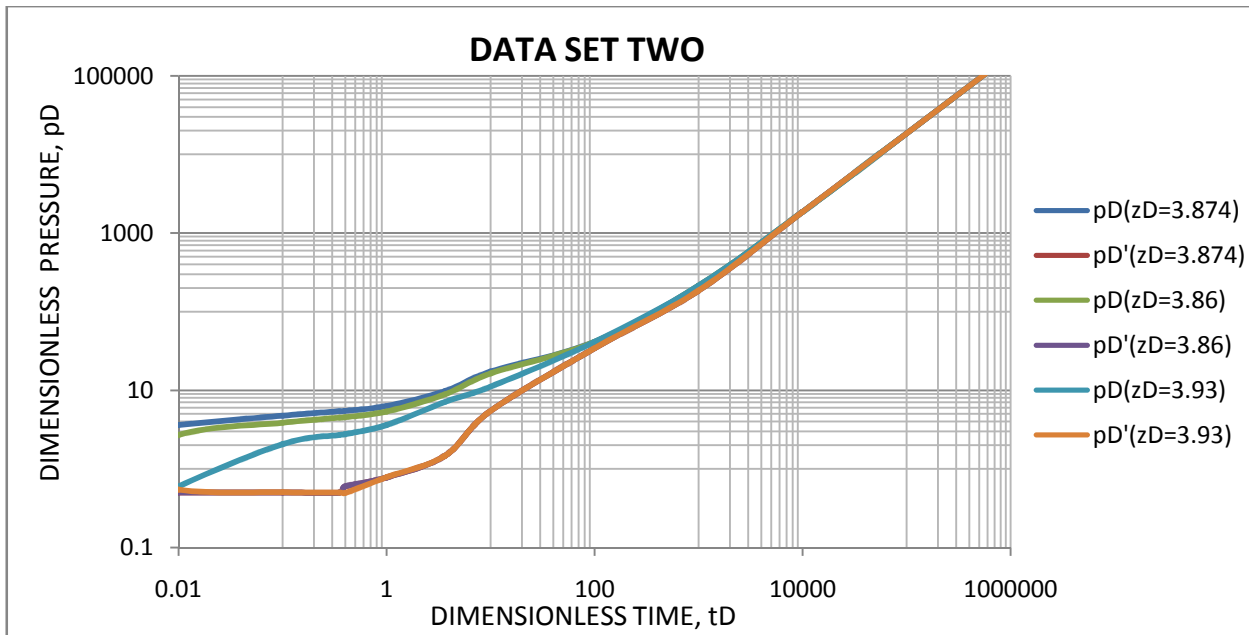


**Figure 2:** Dimensionless Pressure and Dimensionless Pressure Derivative plots for Vertical Point Coordinate Values (Set Two)

It can be observed from the plot of Figure 2 that during the early-time flow, the curves of  $z_D = 3.86$  and  $z_D = 3.874$  are in close proximity to each other and increase infinitely between points  $t_D = 0.001$  and  $t_D = 0.352$ . This behavior of pressure response suggests that the reservoir is infinitely large in size with no flow interference by any boundary. The slope of each of the curves remains unchanged with a constant value of 1.151 during this period. This signifies that the vertical point coordinate has negligible effect on the pressure distribution during the early-time flow between the two curves. It can also be noticed from the plot that at the inception of flow, the dimensionless pressure curve of  $z_D = 3.93$  is conspicuously separated from the other curves during the infinite-acting flow period, with a constantly changing slope. As time increases, this curve gradually comes within the reach of the others. This indicates that the infinite-acting flow period gradually disappears as flow is further away from the well and approaches the boundary. Between  $t_D = 0.352$  and  $t_D = 0.394$ , the reservoir experiences its first transition from the early-time flow signifying the influence of a boundary. At this time, the early-time flow ends and the first transition flow becomes dominant. This flow period indicates that the well has seen the closest boundary either in the  $x$  or  $z$  plane. This flow is characterized by a gradual merging of the dimensionless pressure curves of  $z_D = 3.86$  and  $z_D = 3.874$ . The second transition flow occurs between  $t_D = 0.394$  and  $t_D = 3.647$ . This flow period is characterized by a slight deviation in course from the first transition flow pattern on the dimensionless pressure curves. From the time  $t_D = 3.647$  and upward, pseudo-steady state occurs. It can be seen on the plot, that during this period of flow, all the curves merge with each other and rise steadily with increasing pressure values. This pressure increase indicates that the average reservoir pressure of the reservoir system has started to decrease over time; however, the curves remain unaffected by variation in  $z_D$ .

The dimensionless pressure derivative curves as illustrated on the same graph above shows that for both varied values of  $z_D = 3.86$  and  $z_D = 3.874$ , the curves flatten at an approximately constant value of 0.5 during the early-time flow between  $t_D = 0.001$  and  $t_D = 0.352$ . This is usually the norm for a vertical well pressure distribution. Between the early-time flow and the first transition flow, the curves experience a visible rise as the influence of a boundary is felt. Between the first and second transition flow, there is a slight dip on the curves. These features are clearly visible on the derivative curves because they reveal features that are hidden in the dimensionless pressure curves.

#### 1. Effect Of Lateral Extent ( $x_{eD}$ ) On Pressure Distribution

The effect of the parameter,  $x_{eD}$ , on pressure distribution of a vertical well in a bounded reservoir system was examined by keeping all other parameters constant while varying  $x_{eD}$ .

The reservoir lateral extent being varied for the third set of wellbore and reservoir parameters were taken as  $x_{eD} = 16.52$ ,  $x_{eD} = 20.4$  and  $x_{eD} = 30.6$ . These parameters represent different values of the dimensionless drainage radius.

A plot of the dimensionless pressure and dimensionless pressure derivative results against the dimensionless time is also illustrated in Figure 3 on the log-log axis for the first set of parameters while varying  $x_{eD}$ .

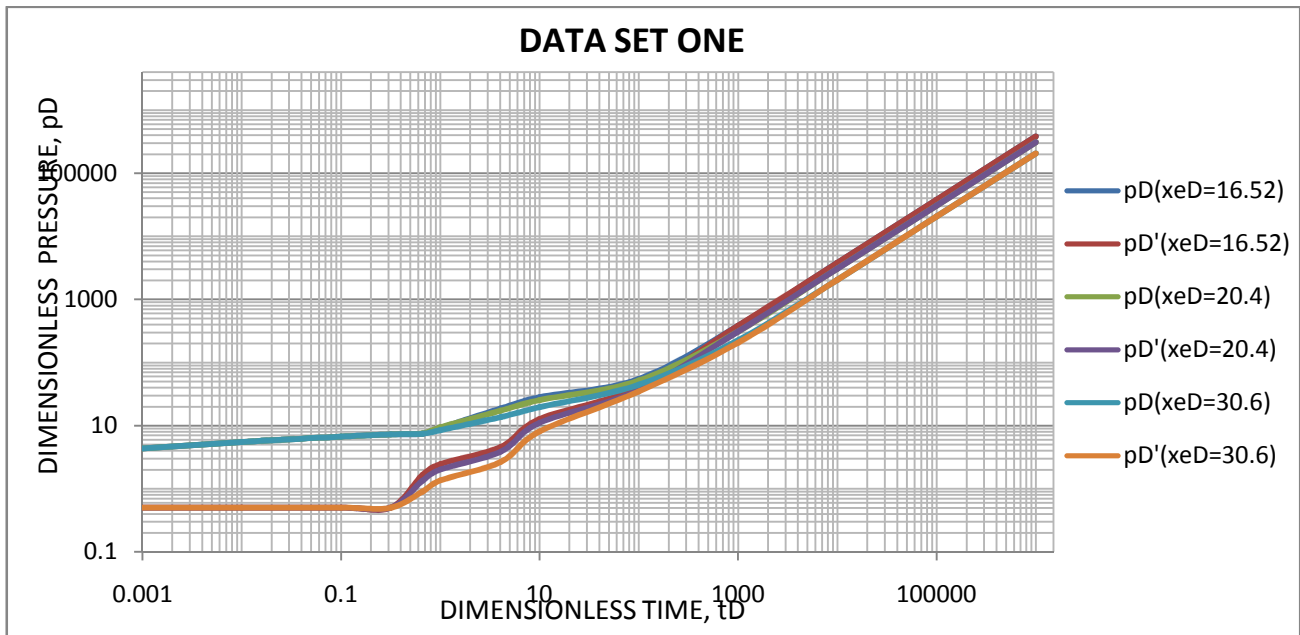


**Figure 3:** Dimensionless Pressure and Dimensionless Pressure Derivative plots for Lateral Extent Values (Set One)

It can be observed from Figure 3 that during the early – time flow, the pressure values remain unchanged for the different values of  $x_{eD}$  being investigated. It shows the curves merging between  $t_D = 0.001$  and  $t_D = 0.318$ . Since the effect of  $x_{eD}$  is unnoticed, it thus means that it has no effect on pressure distribution during the infinite – acting flow period. During this period of flow, the dimensionless pressure curves increase infinitely with time with a slope of 1.151. This is usually the convention for a vertical well pressure distribution. During this period flow which is called infinite – acting flow period, the reservoir behaves as though it is infinite in size with fluid flowing radially into the well bore from all directions. Since the influence of the boundary has not been felt at this time, near wellbore characterization is possible and clean oil production guaranteed. Furthermore, it can be observed that the curves seem to separate apart from each other as the reservoir undergoes its first transition between  $t_D = 0.318$  and  $t_D = 0.439$ . It is observed during this period, that there is an obvious change in the dimensionless pressure as the value of  $x_{eD}$  increases. The curves further separate as the reservoir undergoes another transition, this time, to pseudo – steady state. As can be seen from the curves, the dimensionless pressure distribution tends to reduce as the value of  $x_{eD}$  increases during these periods. The transition periods are desired because they delay, to some extent, the attainment of pseudo – steady state, thereby preventing early rapid depletion of the reservoir. As the transition flow recedes over time, pseudo – steady state flow becomes prevailing, indicating the influence of all boundaries on pressure distribution. It can be observed from the dimensionless curves that the pressure distribution increases rapidly at late – time. However, the rate of depletion decreases as  $x_{eD}$  increases and vice versa.

The reservoir pressure response is quite noticeable in the dimensionless pressure derivative curves because hidden features in the dimensionless pressure curves are clearly revealed. Figure 1 shows that at early – time, the derivative curves stabilize at constant pressure values of 0.5. The merging of the curves during this period, is an indication that  $x_{eD}$  has no effect, whatsoever, on pressure response during the early – time flow. As the infinite – acting flow period gradually disappears, the transition flow becomes dominant with obvious separation of the curves as clearly shown on the pressure derivative curves. This behavior validates the earlier representation on the dimensionless pressure curves as shown in the plot. During the pseudo – steady state flow, it is observed that the dimensionless pressure derivative curves merge characteristically with the dimensionless pressure curves and increase at a constant rate.

The reservoir lateral extent being varied for the second set of wellbore and reservoir parameters were taken as  $x_{eD} = 50.98$ ,  $x_{eD} = 60.69$  and  $x_{eD} = 67.97$ . These parameters represent different values of the dimensionless drainage radius.

### 3. Effect Of Lateral Point Coordinates ( $x_D$ )

The effect of the parameter,  $x_D$ , on pressure distribution of a vertical well in a bounded reservoir system was examined by keeping all other parameters constant while varying  $x_D$ .

The reservoir lateral point coordinates being varied for the third set of wellbore and reservoir parameters were taken as  $x_D = 19.84$ ,  $x_D = 28.86$  and  $x_D = 30.66$ . These parameters represent different points along the lateral coordinate of the reservoir system.

A plot of the dimensionless pressure and dimensionless pressure derivative results against the dimensionless time is also illustrated in Figure 4 on the log-log axis for the second set of parameters while varying  $x_D$ .

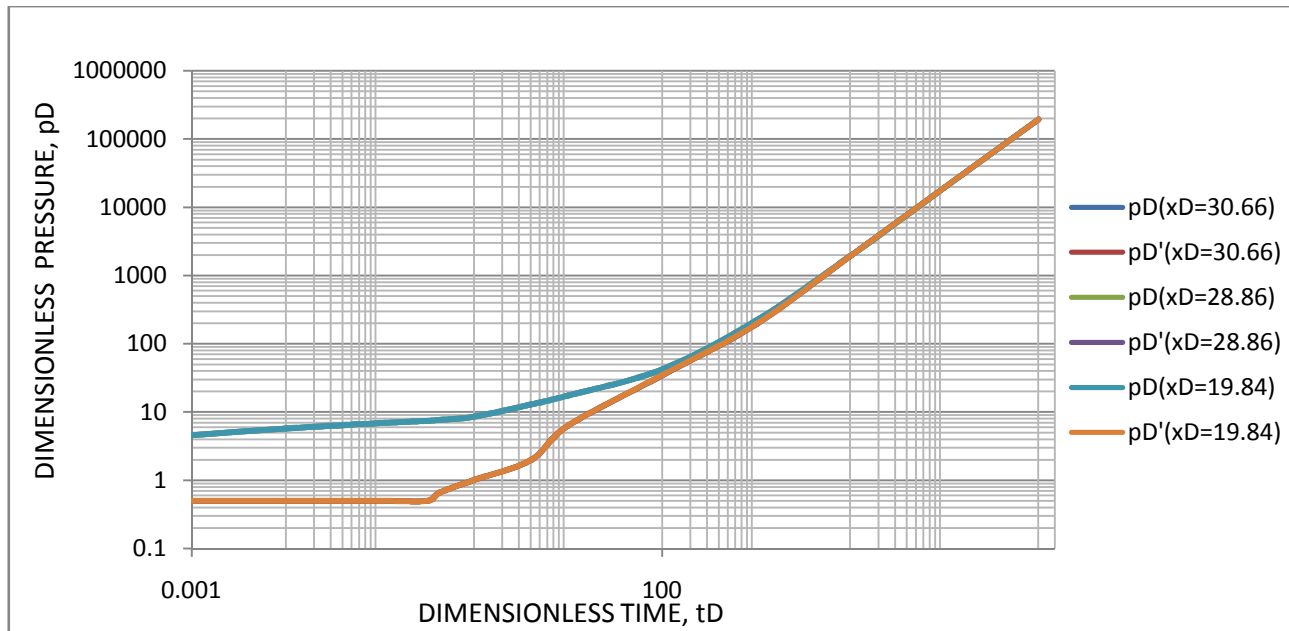


**Figure 4:** Dimensionless Pressure and Dimensionless Pressure Derivative plots for Lateral Point Coordinate Values

On the dimensionless pressure plot, as seen in Figure 4, from early time to late time the curves are seen to rise gradually with no distinct separation between the curves. On the dimensionless pressure derivative plots, at early time, a straight horizontal line trend develops with a value of 0.5, and then gradually rises forming a unit slope straight line at later time. No distinct separation is seen between the curves for the different values of  $x_D$  from early time to late time.

This means that from the early radial flow period (where the reservoir acts as if it is infinite and fluid flows in all directions to the wellbore) to the point where pseudo - steady state is attained (the remaining oil in the reservoir is being drained by the vertical well), the pressure distribution of the reservoir remains similar for all varied values of  $x_D$ .

This is an indication that varying the lateral point coordinate has no significant difference in effect on the pressure response of a vertical well in a bounded reservoir.

## 12.0 Conclusion

The pressure analysis of a vertical well in a bounded reservoir has been studied for proper understanding of the pressure behavior of wells in reservoirs which is hardy for making important reservoir engineering decisions. And the following findings were arrived at:

1. Pressure behavior of a vertical well in a bounded reservoir is affected significantly by the reservoir boundary.
2. The impact of the boundaries on pressure responses occur at late time production. Pressure behaviors at early time production are not affected by the boundaries.
3. Situating the well far away from the boundaries delays the attainment of pseudo – steady state.
4. Infinite – acting flow period is unaffected by the lateral extent of the reservoir. However, reservoir depletion during late time reduces with increasing lateral extent.
5. Pressure behavior is unaffected by the lateral point coordinates throughout all the flow regimes.
6. Infinite – acting flow period subsists for a long time when flow is close to the well bore, thereby making it possible to accurately determine near – well bore characteristics using the conventional analysis procedures such as buildup, drawdown and or any other procedure.

## 13.0 Acknowledgement

The authors thank prof. E.S. Adewole, a professor of petroleum engineering at university of Benin and an expert in reservoir simulation and modeling for his support and supervision during and after the research work.

## 14.0 References

- [1] Kamal, M. M.: Use of Pressure Transients to Describe Reservoir Heterogeneity. *JPT:Trans.AIME*, 267, Vol 31, Issue 08,pp1060 – 1070,(1979).
- [2] Abdassah, Doddy.: *Production Well Test and Pressure Analysis*. Bandung: Yayasan IATMI, 2005.

- [3] Matthews, C. S. and Russel, D. G.: Pressure Buildup and Flow Tests in Wells. Vol 1. New York: Society of Petroleum Engineers of AIME, 1967.
- [4] Fekete Associates Inc.: FAST WellTest Help Guide, 2010.
- [5] Chaudhry, Amanat U.: Oil Well Testing Handbook. USA: Elsevier Inc., 2004.
- [6] Kamal, Medhat M.: Transient Well Testing, Monograph vol 23. Richardson, TX: Society of Petroleum Engineers, 2009.
- [7] Kamal, M. M., Fryder, D. G. and Murray, M. A.: Use of Transient Testing in Reservoir Management. SPE – 28002 – PA, 1995.
- [8] Oloro J., Adewole E. S.: Factors that Affect Pressure Distribution of Horizontal Wells in a Layered Reservoir with Simultaneous Gas – cap and Bottom Water Drive.: Journal of Petroleum and Gas Engineering, Vol. 6, Issue1, pp. 1-9, (January, 2013).
- [9] Owolabi A. F., Olafuyi O. A., Adewole E. S.: Pressure Distribution in a Layered Reservoir with Gas – cap and Bottom Water. Nig. Journal of Technology (NIJOTECH) 31(2): 189 – 198.
- [10] Gringarten, A.C., and Ramey, H.J.: “The use of Source and Green’s Function in solving unsteady – flow problems in reservoirs, (October, 1973), 289-290.
- [11] Al Rbeawi S. and Tiab D.: Transient Pressure Analysis of Horizontal Wells in a Multi – Boundary System. American Journal of Engineering Research (AJER), Volume-02, Issue-04, pp-44-66, (2013).
- [12] Adewole E. S., Olafuyi O. A.: The Use of Source and Green’s Functions to Derive Dimensionless Pressure and Dimensionless Pressure Derivative of a Two – Layered Reservoir Part II: S – Shaped Architecture, April, 2010.
- [13] Odeh, D.K., and Babu, D.K.: “Transient Flow Behavior of Horizontal Wells: Pressure Drawdown and Buildup Analysis,” SPE Formation Evaluation, pp7-15. (March, 1990).
- [14] Goode, P.A., and Thambynayagam, R.K.M.: “Pressure Drawdown and Buildup Analysis of Horizontal Wells in Anisotropic Media,” SPE Formation Evaluation, SPE-14250-PA, Vol 2, Issue 04, (December 1987),
- [15] Yasin Ilfi, B. E.: Pressure Transient Analysis Using Generated Well Test Data from Simulation of Selected Wells in Norne Field. Masters Thesis, NTNU- Trondheim, Norwegian University of Science and Technology, Department of Petroleum Engineering and Applied Geophysics, (May 2012).